MycoKeys

MycoKeys 115: 187–208 (2025)
DOI: 10.3897/mycokeys.115.140683

Research Article

Morphology and phylogeny of two new species within Cordycipitaceae (Hypocreales) from China

Yingling Lu[1,2*], Songyu Li[1,2*], Zuoheng Liu[1,2], Jing Zhao[1,2], Zhiyong Yu[3], Zongli Liang[3], Hailong He[3], Jianhong Li[3], Yun Huang[3], Xinming Li[3], Hong Yu[1,2]

1 *Yunnan Herbal Laboratory, College of Ecology and Environmental Sciences, Yunnan University, Kunming, Yunnan 650504, China*
2 *The International Joint Research Center for Sustainable Utilization of Cordyceps Bioresources in China and Southeast Asia, Yunnan University, Kunming 650091, China*
3 *Yunnan Jinping Fenshuiling National Nature Reserve, Honghe, Yunnan 661500, China*

Corresponding author: Hong Yu (hongyu@ynu.edu.cn, herbfish@163.com)

Abstract

Simplicillium and *Leptobacillium*, sister genera in the family Cordycipitaceae, exhibit a broad range of hosts or substrates. The identification of two novel species, from *Simplicillium* and *Leptobacillium*, was achieved by analysing morphological characteristics and phylogenetic data obtained from six molecular markers (ITS, nrSSU, nrLSU, *tef-1α*, *rpb1* and *rpb2*). The two recently documented species are *S. puwenense* and *L. longiphialidum*. Morphologically, *S. puwenense* possessed slender solitary rod-shaped or columnar phialides with elliptical oval or cylindrical conidia forming small spherical heads at the apex of phialides. On the other hand, *L. longiphialidum* had solitary columnar phialides with elliptic or subspherical apical conidia while other conidia were narrow columnar or fusiform in shape. Phylogenetic analysis revealed that *S. puwenense* formed an independent branch as a sister species to *S. formicae*, whereas *L. longiphialidum* clustered with *L. marksiae* exhibiting stable topological structure. The Bayesian inference posterior probability and the maximum likelihood bootstrap-ratio provided robust statistical evidence, indicating the presence of two novel species within the genera of *Simplicillium* and *Leptobacillium*. The present study contributes to the discovery of species diversity in *Simplicillium* and *Leptobacillium*, while also providing a taxonomic foundation for their rational development and sustainable utilisation.

Key words: *Leptobacillium*, morphology, new taxa, phylogenetic analysis, *Simplicillium*, taxonomy

Academic editor: Marc Stadler
Received: 31 October 2024
Accepted: 25 February 2025
Published: 17 March 2025

Citation: Lu Y, Li S, Liu Z, Zhao J, Yu Z, Liang Z, He H, Li J, Huang Y, Li X, Yu H (2025) Morphology and phylogeny of two new species within Cordycipitaceae (Hypocreales) from China. MycoKeys 115: 187–208. https://doi.org/10.3897/mycokeys.115.140683

Introduction

As was well known, many species in the family Cordycipitaceae Kreisel ex G.H. Sung, Hywel-Jones & Spatafora were entomogenous (Mongkolsamrit et al. 2018; Wang et al. 2020). Amongst them, the genera *Simplicillium* W. Gams & Zare and *Leptobacillium* Zare & W. Gams were sister genera (Zare and Gams 2001, 2016).

In 2001, Zare and Gams established the genus *Simplicillium*, which included *S. lanosoniveum* (J.F.H. Beyma) Zare & W. Gams (type species), *S. lamellicola*

* These authors contributed equally to this work.

(F.E.V. Sm.) Zare & W. Gams, *S. obclavatum* (W. Gams) Zare & W. Gams and *S. wallacei* H.C. Evans. The key distinguishing characteristic of the *Simplicillium* genus was the solitary presence of phialides, with conidia typically adhering to the apex of phialides in chains that resemble spherical, sticky or tile-like structures, ultimately forming octahedral crystals (Zare and Gams 2001). The solitary phialides enabled the distinction between the genus *Simplicillium* and its closely-related genus *Lecanicillium* W. Gams & Zare (Chen et al. 2021). Species belonging to the *Simplicillium* genus exhibited ecological diversity, including their presence in various environments, such as soil, endophytic fungi of plants, rocks and decaying wood (Liu and Cai 2012; Nonaka et al. 2013; Zhang et al. 2017; Crous et al. 2018, 2021). *S. chinense* F. Liu & L. Cai was the first *Simplicillium* species discovered in China (Liu and Cai 2012).

In 2016, the genus *Leptobacillium* was established by Zare and Gams during the revision of the former *Verticillium* Nees section *Albo-erecta*. The name of the genus referred to its characteristic narrow microconidia, with the model species being *L. leptobactrum* (W. Gams) Zare & W. Gams (Zare and Gams 2016). The genus *Leptobacillium* comprised species that exhibited two distinct types of conidia. Individual cells aggregated to form chains, with nearly spherical or elliptical conidia located at the apex of long chains, while narrow cylindrical (rod-shaped) to fusiform conidia were found elsewhere within the chain (Zare and Gams 2016; Leplat et al. 2022). Zare and Gams (2016) initially described *L. leptobactrum*, a species consisting of two varieties, namely *L. leptobactrum* var. *leptobactrum* (W. Gams) Zare & W. Gams and *L. leptobactrum* var. *calidius* Zare & W. Gams, which were distinguished by their optimal growth temperatures. The species of *Leptobacillium* exhibited a wide range of host and substrate diversity, having been isolated from various sources including Lepidoptera insects, fungi, plants, fresh water, murals and rocks (Liu and Cai 2012; Zare and Gams 2016; Gomes et al. 2018; Crous et al. 2018; Sun et al. 2019; Okane et al. 2020). The nematophagous properties of *Leptobacillium* species have been extensively studied (Regaieg et al. 2011; Leplat et al. 2022).

Phylogenetic studies of species in the genera *Simplicillium* and *Leptobacillium* have focused on the nuclear ribosomal internal transcribed spacer region (ITS) and the nuclear ribosomal large subunit (nrLSU). Currently, several other DNA loci are frequently used to study species in the Cordycipitaceae family (Kepler et al. 2017; Wang et al. 2020; Leplat et al. 2022). Based on a phylogenetic analysis, *S. wallacei* was transplanted into the genus *Lecanicillium* and later Zhang et al. placed *L. wallacei* in the genus *Gamszarea* Z.F. Zhang & L. Cai (Zare and Gams 2001, 2008; Zhang et al. 2021). Phylogenetic analysis, based on five locus data, showed that *S. coffeanum* A.A.M. Gomes & O.L. Pereira, *S. chinensis* F. Liu & L. Cai and *S. filiforme* R.M.F. Silva, R.J.V. Oliveira, Souza-Motta, J.L. Bezerra & G.A. Silva were transferred to the genus *Leptobacillium* (Zare and Gams 2008; Okane et al. 2020; Chen et al. 2021).

Based on a comparative analysis of morphological characteristics and a multigene molecular phylogeny, we characterised in this study two newly-identified species from China, namely *S. puwenense* Hong Yu bis, Y.L. Lu & J. Zhao, sp. nov., from the genus of *Simplicillium* and *L. longiphialidum* Hong Yu bis, Y.L. Lu & J. Zhao, sp. nov., from the genus of *Leptobacillium*, respectively. This investigation has contributed to the expansion of the species diversity within the genera of *Simplicillium* and *Leptobacillium*, providing a solid taxonomic foundation to facilitate the rational development and sustainable use of these valuable resources.

Material and method

Material collection and isolation

The specimens of a dead spider infected with fungi were collected in China. One specimen was collected from Puwen Town, Jinghong City, Xishuangbanna Dai Autonomous Prefecture, Yunnan Province, China and the Xilong Mountains in Jinping County, Honghe Hani and Yi Autonomous Prefecture, Yunnan Province, China. Another was collected from Limushan National Forest Park, Limushan Town, Qiongzhong City, Hainan Province, China and 511 Township Road, Boluo County, Huizhou City, Guangdong Province, China. The specimens were photographed, assigned numbers and their collection details including habitat, elevation, latitude and longitude were documented. Subsequently, they were placed in freezing tubes within a vehicle-mounted refrigerator set at 4 °C for transportation back to the laboratory. Upon arrival at the laboratory, the specimens underwent initial observation and measurement using an Optec SZ660 stereo dissecting microscope. A select number of fungal conidia were then carefully picked with an inoculation needle and inoculated into PDA solid medium containing 0.05 g tetracycline and 0.1 g streptomycin using the plate streak method (Wang et al. 2020). The pure culture was incubated at a temperature of 25 °C, while the purified strain was transferred to a bevelled test tube containing PDA medium and stored at 4 °C (Wang et al. 2020). The specimens were deposited in the Yunnan Herbal Herbarium (YHH), while the strains were conserved in the Yunnan Fungal Culture Collection (YFCC).

Morphological observations

The pure cultures were transferred to PDA solid medium and incubated at 25 °C for 14 days. Colony diameters were measured, colony characteristics were recorded and photographs of the front and back of the colonies were captured using a Canon camera (Tokyo, Japan). To observe the microscopic morphology of the colonies, filter paper was cut to fit a petri dish and placed inside. A U-shaped glass shelf, a slide and two coverlids that had been sterilised at 121 °C for 30 minutes and then dried were prepared. A layer of PDA medium with a thickness of 1 mm and size of approximately 5 mm was applied onto the slide. A small amount of mycelia was selected from each culture and transferred to the centre of the medium. It was covered with a coverslip, sterile water was added to moisten the medium and sealed in an incubator at 25 °C for cultivation. The microstructure was observed, measured and photographed using fluorescence microscopes CX40 (Tokyo, Japan) and BX53 (Tokyo, Japan).

DNA extraction, polymerase chain reaction (PCR) and sequencing

The total genomic DNA of fungi was extracted using the CTAB method described by Liu et al. (2001). The ITS region was amplified using primer pairs ITS4 and ITS5 (White et al. 1990). The nuclear ribosomal small subunit (nrSSU) and nrLSU were amplified using primer pairs nrSSU-CoF with nrSSU-CoR and LR5 with LR0R, respectively (Vilgalys and Hester 1990; Rehner and Samuels 1994; Wang et al. 2015b). The translation elongation factor 1α (*tef-1α*) was amplified using primer pairs EF1α-EF and EF1α-ER (Bischoff et al. 2006; Sung et al.

2007). Finally, the largest subunit of RNA polymerase II (*rpb1*) and the second largest subunit of RNA polymerase II (*rpb2*) were amplified using primer pairs RPB1-5'F with RPB1-5'R and RPB2-5'F with RPB2-5'R, respectively, as described by Bischoff et al. (2006) and Sung et al. (2007).

The final volume of all PCR reactions was 25 µl, consisting of 17.25 µl of sterile deionised water, 2.5 µl of PCR10 Buffer (2 mmol/l Mg^{2+}) from Transgen Biotech in Beijing, China, 2 µl of dNTP (2.5 mmol/l), 1 µl each of forward and reverse primers, 0.25 µl of Taq DNA polymerase from Transgen Biotech in Beijing, China and 1 µl of DNA template. The polymerase chain reaction (PCR) for the five genes and ITS was conducted using a BIO-RAD T100TM thermal cycler manufactured by BIO-RAD Laboratories in Hercules, CA, United States (Bischoff et al. 2006; Wang et al. 2015a). The PCR products were analysed through electrophoresis on a 1.0% agarose gel and subsequently stored at -20 °C until they were dispatched in dry ice to BGI Co., Ltd, Shenzhen, China for sequencing.

Phylogenetic analyses

After aligning the six-gene sequences of related species obtained from GenBank with those of the present study using the Clustal W programme in MEGA v.5.0 software, we concatenated the six-gene datasets (ITS, nrSSU, nrLSU, *tef-1α*, *rpb1* and *rpb2*) into a combined matrix comprising all six genes. To both single gene and six-gene datasets, we respectively employed the ModelFinder programme in PhyloSuite v.1.2.2 software to determine the optimal model for the maximum likelihood analysis, based on Corrected AIC (AICc) and IQ-TREE model selection methods. The remaining parameters were set to their default values. Subsequently, we utilised the IQ-TREE programme with 5,000 bootstrap replicates to construct a maximum likelihood tree while selecting appropriate optimal model parameters.

The ModelFinder programme in PhyloSuite v.1.2.2 software was utilised to determine the optimal model for the Bayesian inference using Corrected AIC (AICc) and the MrBayes model, while keeping default settings for other parameters. Subsequently, the MrBayes programme was employed to select appropriate optimal model parameters and run for 2,000,000 generations to construct the BI tree. The constructed phylogenetic trees were visualised in FigTree v.1.4.2 to figure the maximum likelihood method of bootstrap proportion (BP) and the Bayesian inference posterior probability (BPP) and then formatted for editing with Adobe Illustrator CS6.

Results

Phylogenetic analyses

Phylogenetic analysis of single gene molecular fragments

Using single gene fragments of ITS, nrSSU, nrLSU, *tef-1α* and *rpb1* were used to construct *Simplicillium* and *Leptobacillium* phylogenetic trees, respectively. *Beauveria bassiana* ARSEF 1564 and *B. brongniartii* ARSEF 617 were employed as outgroups (Table 1). Among them, the ITS matrix had 64 sequences, 711 bp of bases, including 783 columns, 381 distinct patterns, 218 parsimony-informative,

Table 1. Relevant species information and GeneBank accession numbers for phylogenetic research in this study.

Species	Strain	ITS	nrSSU	nrLSU	*tef-1α*	*rpb1*	*rpb2*	Reference
Beauveria bassiana	ARSEF 1564	HQ880761	-	AF373871	HQ880974	HQ880833	HQ880905	Rehner et al. (2011)
Beauveria brongniartii	ARSEF 617	HQ880782	AB027335	-	HQ880991	HQ880854	HQ880926	Rehner et al. (2011)
Leptobacillium cavernicola	LRMH C212	OM622523	OM628842	OM628781	OM654332	OM677781	OM654321	Leplat et al. (2022)
Leptobacillium cavernicola	LRMH C216	OM622524	OM628843	OM628782	OM654333	OM677782	OM654322	Leplat et al. (2022)
Leptobacillium chinense	CGMCC 3.14969	JQ410323	-	JQ410321	-	-	-	Okane et al. (2020)
Leptobacillium chinense	CGMCC 3.14970	JQ410324	-	JQ410322	-	-	-	Okane et al. (2020)
Leptobacillium coffeanum	COAD 2057	MF066034	-	MF066032	-	-	-	Okane et al. (2020)
Leptobacillium coffeanum	COAD 2061	MF066035	-	MF066033	-	-	-	Okane et al. (2020)
Leptobacillium filiforme	URM 7918	-	-	MH979399	-	-	-	Okane et al. (2020)
Leptobacillium latisporum	TBRC 16288	OP856540	OP850838	OP856529	-	-	-	Preedanon et al. (2023)
Leptobacillium leptobactrum	ZJ14B02	PP385689	-	PP381743	-	-	-	Unpublished
Leptobacillium leptobactrum	AH17C05	PP384754	-	PP380808	-	-	-	Unpublished
Leptobacillium leptobactrum var. *calidius*	CBS 703.86	EF641866	EF641850	KU382226	-	-	-	Zare and Gams (2016)
Leptobacillium leptobactrum var. *leptobactrum*	CBS 771.69	EF641868	EF641852	KU382224	-	-	-	Zare and Gams (2016)
Leptobacillium longiphialidum	**YFCC 23039272^{T}**	**PQ509282**	**PQ508806**	**PQ508808**	**PQ560997**	**PQ567240**	-	**This study**
Leptobacillium longiphialidum	**YFCC 24079491**	**PQ509281**	**PQ508805**	**PQ508807**	**PQ560996**	**PQ567239**	-	**This study**
L. marksiae	BRIP 70307a	PQ061114	-	PQ047739	-	-	-	Tan and Bishop-Hurley (direct submission)
Leptobacillium muralicola	CGMCC 3.19014	MH379983	-	MH379997	-	-	-	Sun et al. (2019)
Leptobacillium muralicola	CGMCC 3.19015	MH379985	-	MH379999	-	-	-	Sun et al. (2019)
Leptobacillium symbioticum	NBRC 113865	LC485673	-	LC506046	-	-	-	Okane et al. (2020)
Leptobacillium symbioticum	OPTF00168	LC485675	-	LC506047	-	-	-	Okane et al. (2020)
Simplicillium album	LC12442	-	-	-	MK336068	-	-	Zhang et al. (2021)
Simplicillium aogashimaense	JCM 18167	AB604002	-	LC496874	LC496904	-	-	Nonaka et al. (2013)
Simplicillium aogashimaense	JCM 18168	AB604004	-	LC496875	-	-	-	Nonaka et al. (2013)
Simplicillium araneae	DY101811	OM743774	-	OM743792	OM818465	-	-	Chen et al. (2022)
Simplicillium araneae	DY101812	OM743840	-	OM743846	OM818466	-	-	Chen et al. (2022)
Simplicillium calcicola	LC5586	KU746706	-	KU746752	KX855252	-	-	Zhang et al. (2017)
Simplicillium calcicola	LC5371	KU746705	-	KU746751	KX855251	-	-	Zhang et al. (2017)
Simplicillium cicadellidae	GY11012	MN006244	-	-	MN022264	MN022272	-	Chen et al. (2019)
Simplicillium cicadellidae	GY11011	MN006243	-	-	MN022263	MN022271	-	Chen et al. (2019)
Simplicillium coccinellidae	DY101791	MT453861	MT453863	-	MT471341	-	-	Chen et al. (2021)
Simplicillium coleopterorum	SD05381	OM743920	-	OM743925	OM818467	-	-	Chen et al. (2022)
Simplicillium coleopterorum	SD05382	OM744109	-	OM744170	OM818468	-	-	Chen et al. (2022)
Simplicillium cylindrosporum	JCM 18169	AB603989	-	LC496876	LC496906	-	-	Nonaka et al. (2013)
Simplicillium cylindrosporum	JCM 18170	AB603994	-	LC496877	LC496907	-	-	Nonaka et al. (2013)
Simplicillium formicae	DY09641	OR121054	-	OR121057	OR126571	-	-	Unpublished
Simplicillium formicae	DY09642	OR121055	-	OR121056	OR126572	-	-	Unpublished
Simplicillium guizhouense	DY10051	OM743225	-	OM743226	OM818453	-	-	Chen et al. (2022)
Simplicillium guizhouense	DY10052	OM743241	-	OM743252	OM818454	-	-	Chen et al. (2022)
Simplicillium humicola	LC 12494	-	-	-	MK336072	-	-	Zhang et al. (2021)
Simplicillium humicola	CGMCC 3.19573	NR_172845	-	MK329041	MK336071	-	-	Unpublished
Simplicillium hymenopterorum	DY101692	MT453851	-	-	MT471338	-	-	Unpublished
Simplicillium hymenopterorum	DY101691	MT453848	MT453849	-	MT471337	MT471344	-	Unpublished
Simplicillium lamellicola	JC-1	MT807906	MT807908	MT807907	-	-	-	Unpublished

Species	Strain	ITS	nrSSU	nrLSU	*tef-1α*	*rpb1*	*rpb2*	Reference
Simplicillium lamellicola	CBS 116.25	AJ292393	-	-	DQ522356	DQ522404	DQ522462	Nonaka et al. (2013)
Simplicillium lanosoniveum	CBS 704.86	AJ292396	-	-	DQ522358	DQ522406	DQ522464	Nonaka et al. (2013)
Simplicillium larvatum	DY101731	OM743438	-	OM743441	OM818462	OM818460	-	Chen et al. (2022)
Simplicillium lepidopterorum	GY29132	MN006245	-	-	MN022266	MN022274	-	Chen et al. (2019)
Simplicillium lepidopterorum	GY29131	MN006246	-	-	MN022265	MN022273	-	Chen et al. (2019)
Simplicillium minatense	JCM 18176	AB603992	LC496893	LC496878	LC496908	-	-	Nonaka et al. (2013)
Simplicillium minatense	JCM 18178	AB603993	LC496894	LC496879	LC496909	-	-	Nonaka et al. (2013)
Simplicillium neolepidopterorum	DY101752	MT453857	-	-	MT471340	-	-	Chen et al. (2021)
Simplicillium neolepidopterorum	DY101751	MT453854	MT453856	-	MT471339	-	-	Chen et al. (2021)
Simplicillium obclavatum	CBS 311.74	AJ292394	-	AF339517	EF468798	-	-	Nonaka et al. (2013)
Simplicillium obclavatum	SUF81	-	-	MK788174	-	-	-	Unpublished
Simplicillium pechmerlense	CBS 147188	MW031272	-	MW031268	MW033224	MW033222	-	Leplat et al. (2021)
Simplicillium puwenense	**YFCC 23129490^{T}**	**PQ508796**	**PQ508799**	**PQ508802**	**PQ537122**	**PQ560994**	-	**This study**
Simplicillium puwenense	**YFCC 23089322**	**PQ508797**	**PQ508800**	**PQ508803**	**PQ537123**	-	-	**This study**
Simplicillium puwenense	**YFCC 23069492**	**PQ508798**	**PQ508801**	**PQ508804**	**PQ537124**	**PQ560995**	-	**This study**
Simplicillium scarabaeoidea	DY101392	MT453845	-	-	MT471336	-	-	Chen et al. (2021)
Simplicillium scarabaeoidea	DY101391	MT453842	MT453843	-	MT471335	MT471343	-	Chen et al. (2021)
Simplicillium sinense	AFMCCC 16a	OQ332403	-	-	OQ352167	-	-	Yan et al. (2023)
Simplicillium sinense	AFMCCC 16b	OQ332404	-	-	OQ352168	-	-	Yan et al. (2023)
Simplicillium spumae	JCM 39054	LC496871	-	LC496887	LC496917	-	-	Kondo et al. (2020)
Simplicillium spumae	JCM 39050	LC496869	LC496898	LC496883	LC496913	-	-	Kondo et al. (2020)
Simplicillium subtropicum	JCM 18180	AB603990	-	LC496880	LC496910	-	-	Nonaka et al. (2013)
Simplicillium subtropicum	JCM 18181	AB603995	-	LC496881	LC496911	-	-	Nonaka et al. (2013)
Simplicillium sympodiophorum	JCM 18184	AB604003	-	LC496882	LC496912	-	-	Nonaka et al. (2013)
Simplicillium yunnanense	YFCC 7134	-	MN576729	MN576785	MN576955	MN576845	-	Wang et al. (2020)
Simplicillium yunnanense	YFCC 7133	-	MN576728	MN576784	MN576954	MN576844	-	Wang et al. (2020)

64 singleton sites, 500 constant sites. The Best-fit model of the ML tree constructed by the ITS matrix was TIM2+F+I+G4 and the BI tree was GTR+F+I+G4 (Fig. 1). The nrSSU matrix consisted of 21 sequences, 1,122 bp of bases, 2,333 columns, 163 distinct patterns, 30 parsimony-informative, 48 singleton sites and 2,255 constant sites. The Best-fit model for building the nrSSU ML tree was TIM3e+I and the BI tree was SYM+I (Fig. 2). The nrLSU had 52 sequences with 1,126 columns, 325 distinct patterns, 91 parsimony-informative, 340 singleton sites, 695 constant sites and 1,019 bp bases. Based on ML and BI, the Best-fit models used to construct the nrLSU phylogenetic framework were K2P+R5, GTR+F+G4, respectively (Fig. 3). The *tef-1α* matrix consists of 52 sequences, 1,090 columns, 431 distinct patterns, 289 parsimony-informative, 82 singleton sites, 719 constant sites and 1,154 bp bases. The Best-fit model of the ML tree constructed by the *tef-1α* matrix was TIM3+F+R8 and the BI tree was GTR+F+I+G4 (Fig. 4). The *rpb1* matrix consisted of 20 sequences, 803 bp bases, 2,971 columns, 390 distinct patterns, 294 parsimony-informative, 113 singleton sites and 2,564 constant sites. Based on ML and BI, the Best-fit models used to construct the *rpb1* phylogenetic framework were TIM2e+I+G4, SYM+I+G4, respectively (Fig. 5). The tree shapes constructed, based on ML and BI, were

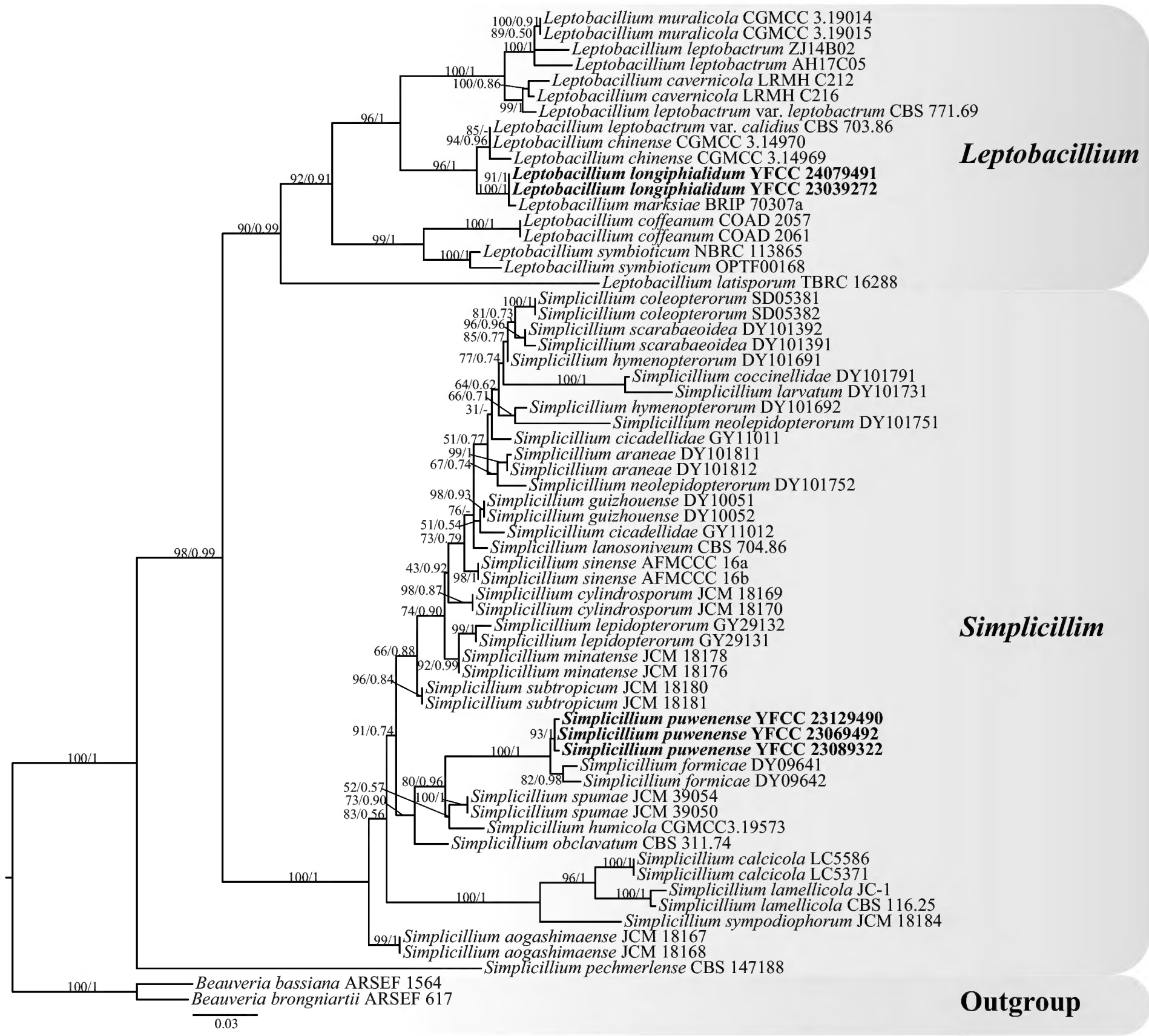

Figure 1. The phylogenetic tree of *Simplicillium* and *Leptobacillium* was inferred from ITS sequence, based on the Bayesian inference and the maximum likelihood analyses. Each value at a node indicates a bootstrap proportion (the left) and Bayesian posterior probability (the right). The scale bar 0.03 indicates the number of expected mutations per site. The species in bold black font of the *Simplicillium* and *Leptobacillium* were from this study. *B. bassiana* ARSEF 1564 and *B. brongniartii* ARSEF 617 were designated as outgroups.

basically the same and the topological structure adopted in this study was a phylogenetic tree constructed by the maximum likelihood method (Figs 1–5).

Based on the phylogenetic framework constructed by single gene fragments, it was found that the resulting topologies were roughly similar and there was no obvious conflict between different gene fragments. The species *S. puwenense* and *L. longiphialidum* collected and described in this study were located in roughly the same position in each phylogenetic tree, forming monophyletic, with high support rate and stable topological structure. In the topology constructed, based on ITS, nrLSU and *tef-1α* matrices, *S. puwenense* and *S. formicae* D.P. Wei & K.D. Hyde were closely related. In phylogenetic trees constructed by ITS and nrLSU matrices, *L. longiphialidum* and *L. marksiae* Tan, Bishop-Hurley & Marney came together.

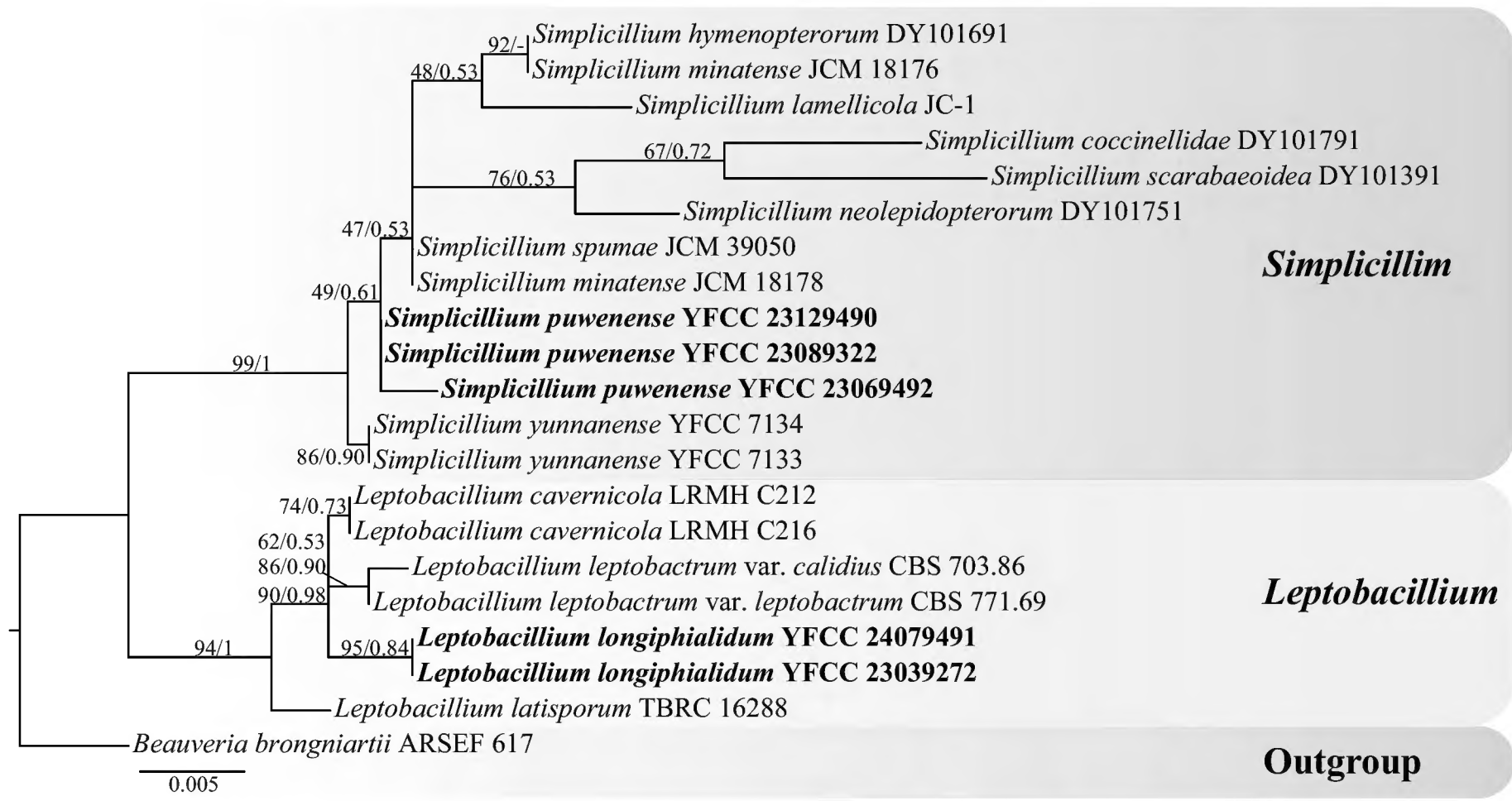

Figure 2. The phylogenetic tree of *Simplicillium* and *Leptobacillium* was inferred from nrSSU sequence, based on the Bayesian inference and the maximum likelihood analyses. Each value at a node indicates a bootstrap proportion (the left) and Bayesian posterior probability (the right). The scale bar 0.005 indicates the number of expected mutations per site. The species in bold black font of the *Simplicillium* and *Leptobacillium* were from this study. *B. brongniartii* ARSEF 617 was designated as outgroup.

Phylogenetic tree reconstructed from multi-gene combined dataset

The phylogenetic framework for the genera *Simplicillium* and *Leptobacillium*, comprising 70 taxonomic units, was constructed, based on a six-gene dataset utilising the maximum likelihood method and Bayesian inference. *B. bassiana* ARSEF 1564 and *B. brongniartii* ARSEF 617 were employed as outgroups (Table 1). The joint matrix comprised 14,494 columns, 1,873 distinct patterns, 1,190 parsimony-informative, 770 singleton sites and 12,534 constant sites. The most appropriate model for the ML analysis amongst the 286 models simulated by ModelFinder was TIM2+F+R10, which achieved an IQ-TREE best score of -32893.153 and a Total tree length of 2.122. The parameters of the TIM2+F+R10 model used to analyse the dataset were estimated, based on the following nucleotide frequencies: A = 0.243, C = 0.262, G = 0.261, T = 0.233, A–C = 1.15866, A–G = 2.32357, A–T = 1.15866, C–G = 1.00000, C–T = 5.27826 and G–T = 1.00000. The GTR+F+I+G4 model was determined as the most suitable model for the BI analysis using ModelFinder amongst the 24 simulated models. It achieved an IQ-TREE best score of -33090.992 and a total tree length of 1.634. The phylogenetic trees constructed using the maximum likelihood (ML) and the Bayesian inference (BI) methods exhibited a high degree of similarity, as depicted in Fig. 6.

The phylogenetic tree of the six-gene joint dataset revealed that the majority of species were grouped in distinct branches with robust support, indicating a stable topology (Fig. 6). The strains YFCC 23129490, YFCC 23069492 and YFCC 23089322, collected and described in this study, formed a well-supported single branch. *S. puwenense* and *S. formicae* were identified as sister species, constituting an independent clade with BP and BPP values of 100% and 1, respectively, while maintaining topological stability. YFCC 24079491 and

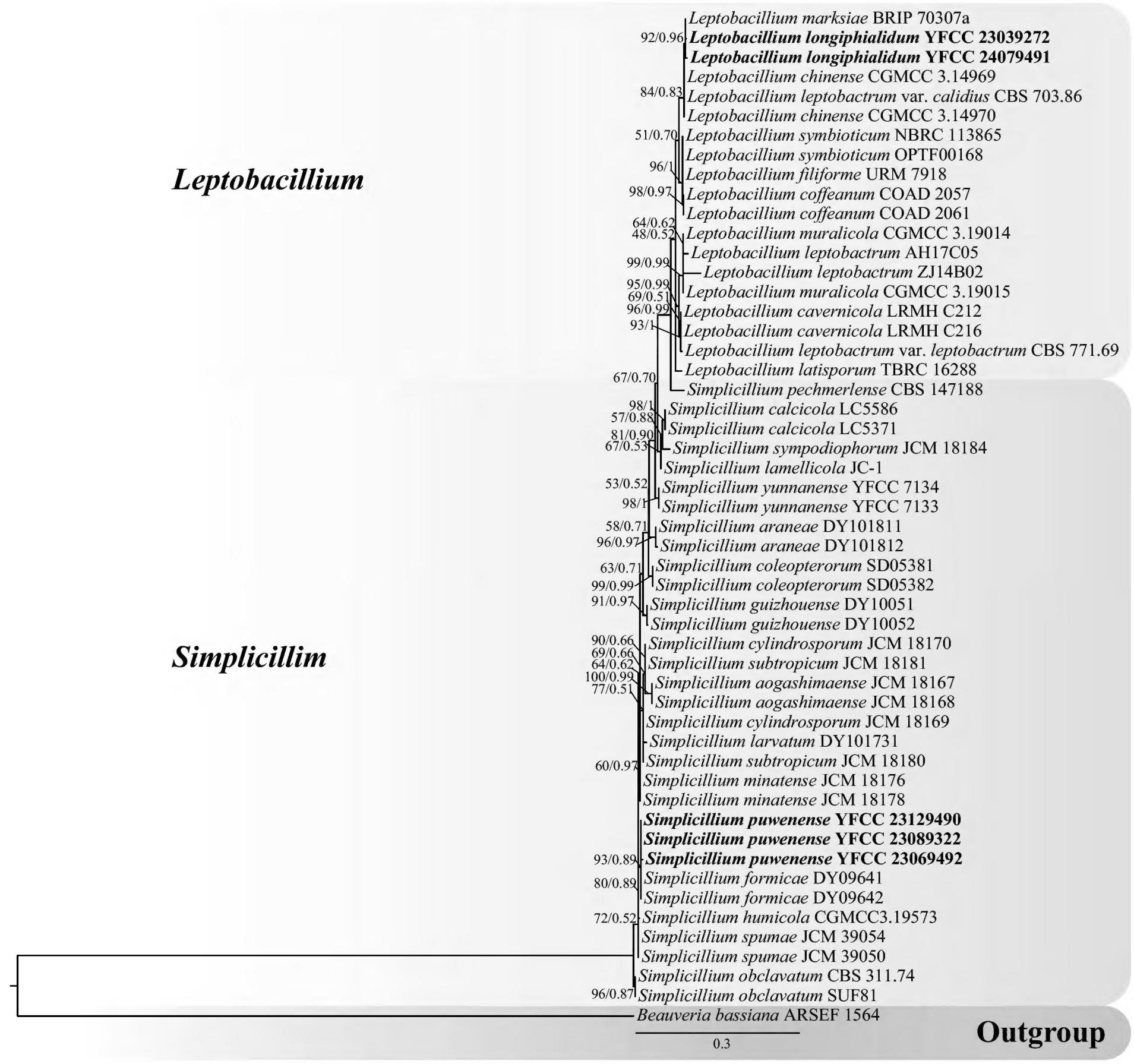

Figure 3. The phylogenetic tree of *Simplicillium* and *Leptobacillium* was inferred from nrLSU sequence, based on the Bayesian inference and the maximum likelihood analyses. Each value at a node indicates a bootstrap proportion (the left) and Bayesian posterior probability (the right). The scale bar 0.3 indicates the number of expected mutations per site. The species in bold black font of the *Simplicillium* and *Leptobacillium* were from this study. *B. bassiana* ARSEF 1564 was designated as outgroup.

YFCC 23039272 clustered together (BP = 100%, BPP = 1). *L. longiphialidum* and *L. marksiae* clustered into a clade, with BP and BPP of 97% and 1, respectively, forming sister species and receiving high support.

Taxonomy

***Simplicillium puwenense* Hong Yu bis, Y.L. Lu & Jing Zhao, sp. nov.**

MycoBank No: 856314

Fig. 7

Etymology. Named after the location Puwen Town where the pattern material was collected.

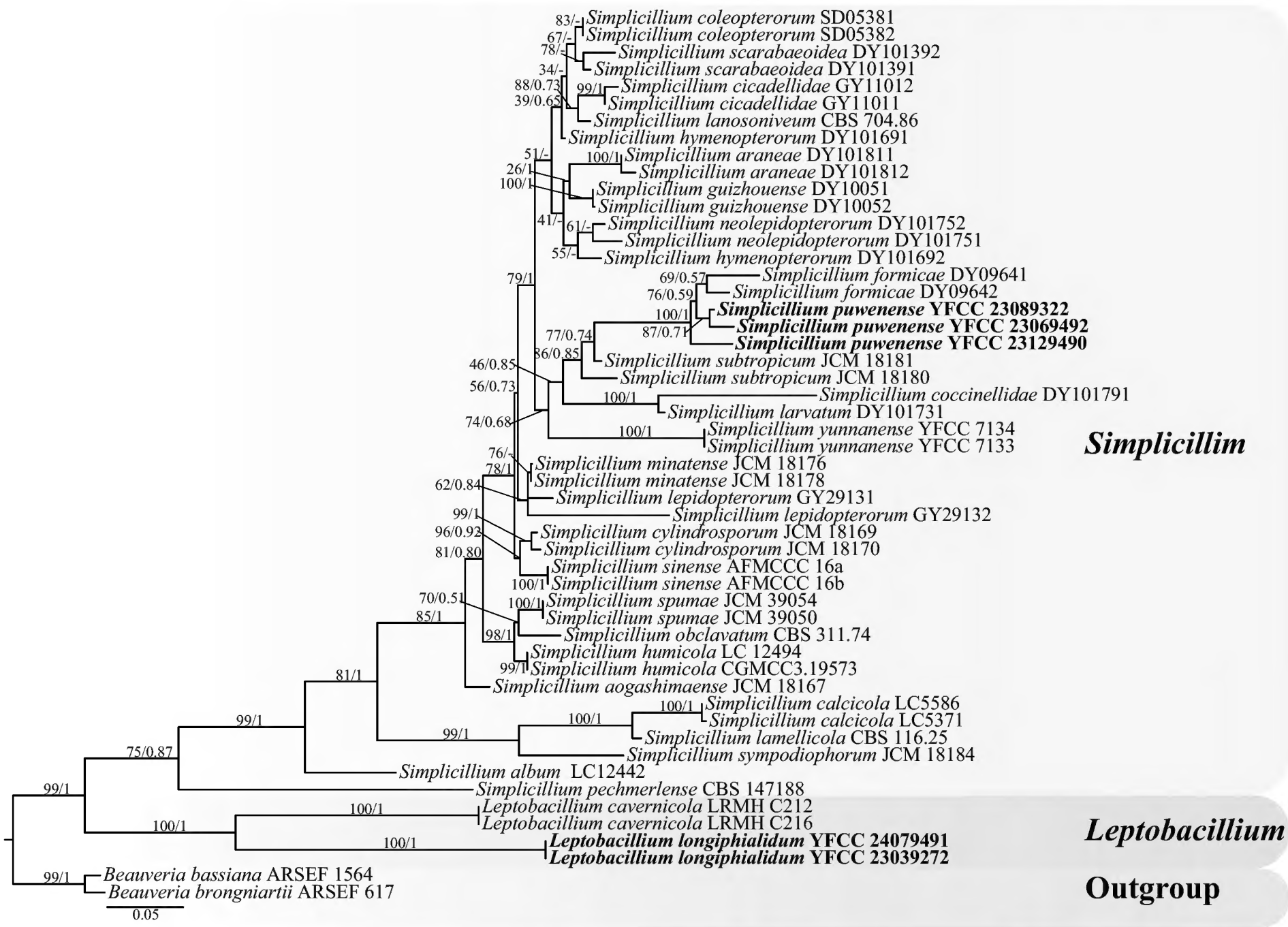

Figure 4. The phylogenetic tree of *Simplicillium* and *Leptobacillium* was inferred from *tef-1α* sequence, based on the Bayesian inference and the maximum likelihood analyses. Each value at a node indicates a bootstrap proportion (the left) and Bayesian posterior probability (the right). The scale bar 0.05 indicates the number of expected mutations per site. The species in bold black font of the *Simplicillium* and *Leptobacillium* were from this study. *B. bassiana* ARSEF 1564 and *B. brongniartii* ARSEF 617 were designated as outgroups.

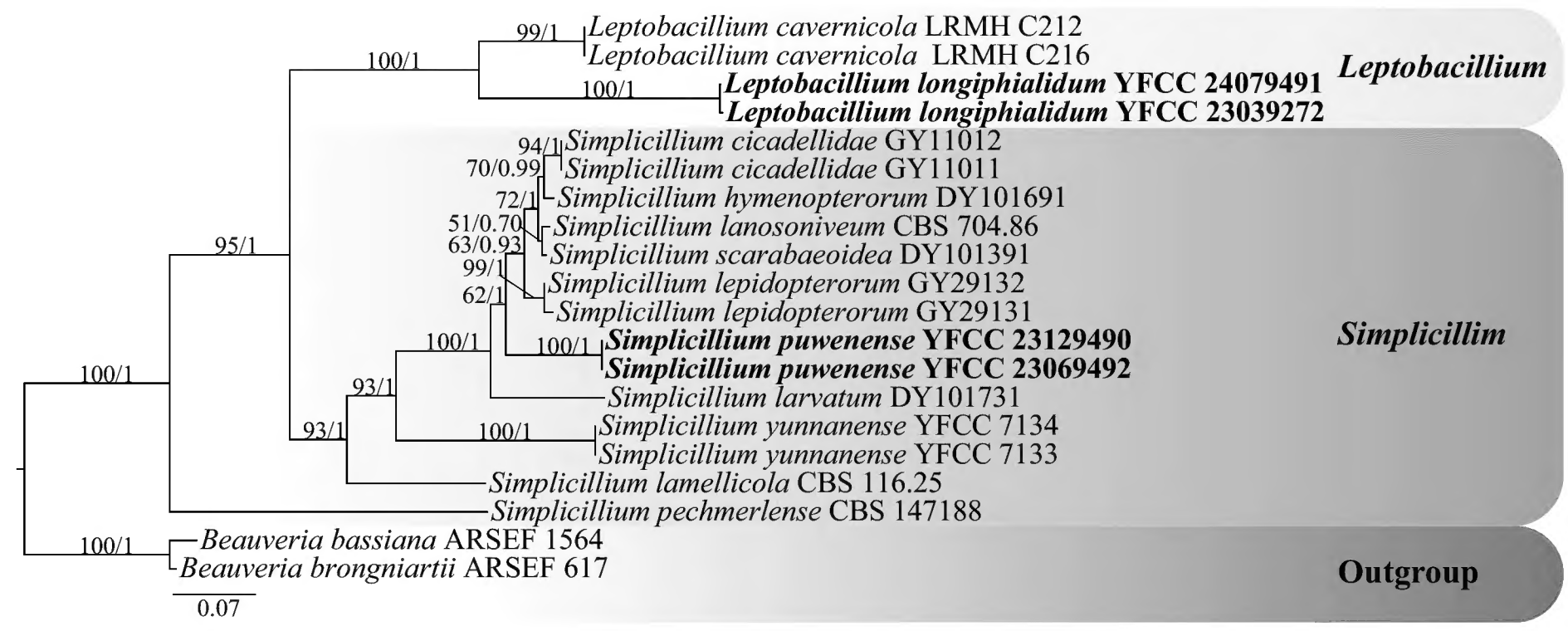

Figure 5. The phylogenetic tree of *Simplicillium* and *Leptobacillium* was inferred from *rpb1* sequence, based on the Bayesian inference and the maximum likelihood analyses. Each value at a node indicates a bootstrap proportion (the left) and Bayesian posterior probability (the right). The scale bar 0.07 indicates the number of expected mutations per site. The species in bold black font of the *Simplicillium* and *Leptobacillium* were from this study. *B. bassiana* ARSEF 1564 and *B. brongniartii* ARSEF 617 were designated as outgroups.

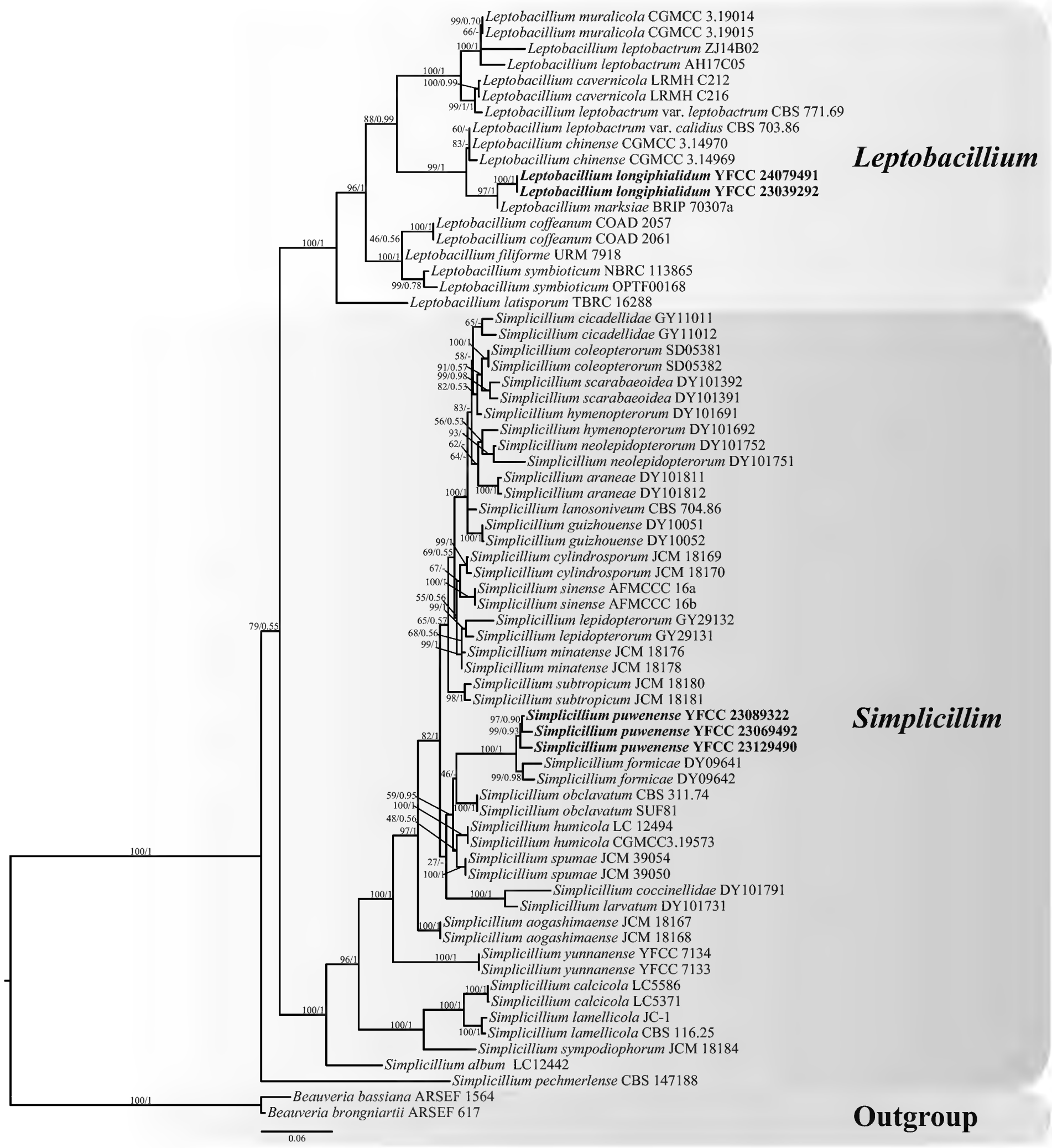

Figure 6. The phylogenetic tree of *Simplicillium* and *Leptobacillium* was inferred from six-gene dataset (ITS, nrSSU, nrLSU, *tef-1α*, *rpb1*, *rpb2*), based on the Bayesian inference and the maximum likelihood analyses. Each value at a node indicates a bootstrap proportion (the left) and Bayesian posterior probability (the right). The scale bar 0.06 indicates the number of expected mutations per site. The species in bold black font of the *Simplicillium* and *Leptobacillium* were from this study. *B. bassiana* ARSEF 1564 and *B. brongniartii* ARSEF 617 were designated as outgroups.

Holotype. China • Yunnan Province, Xishuangbanna Dai autonomous prefecture, Jinghong City, Puwen Town. Specimens were collected from an evergreen broad-leaved forest, alt. 1,062 m, 100°58'60"E, 22°31'20"N, 13 December 2023, Hong Yu (***holotype*:** YHH SP2312001, ***ex-type living culture*:** YFCC 23129490).

Description. *Sexual morph*. Not found.

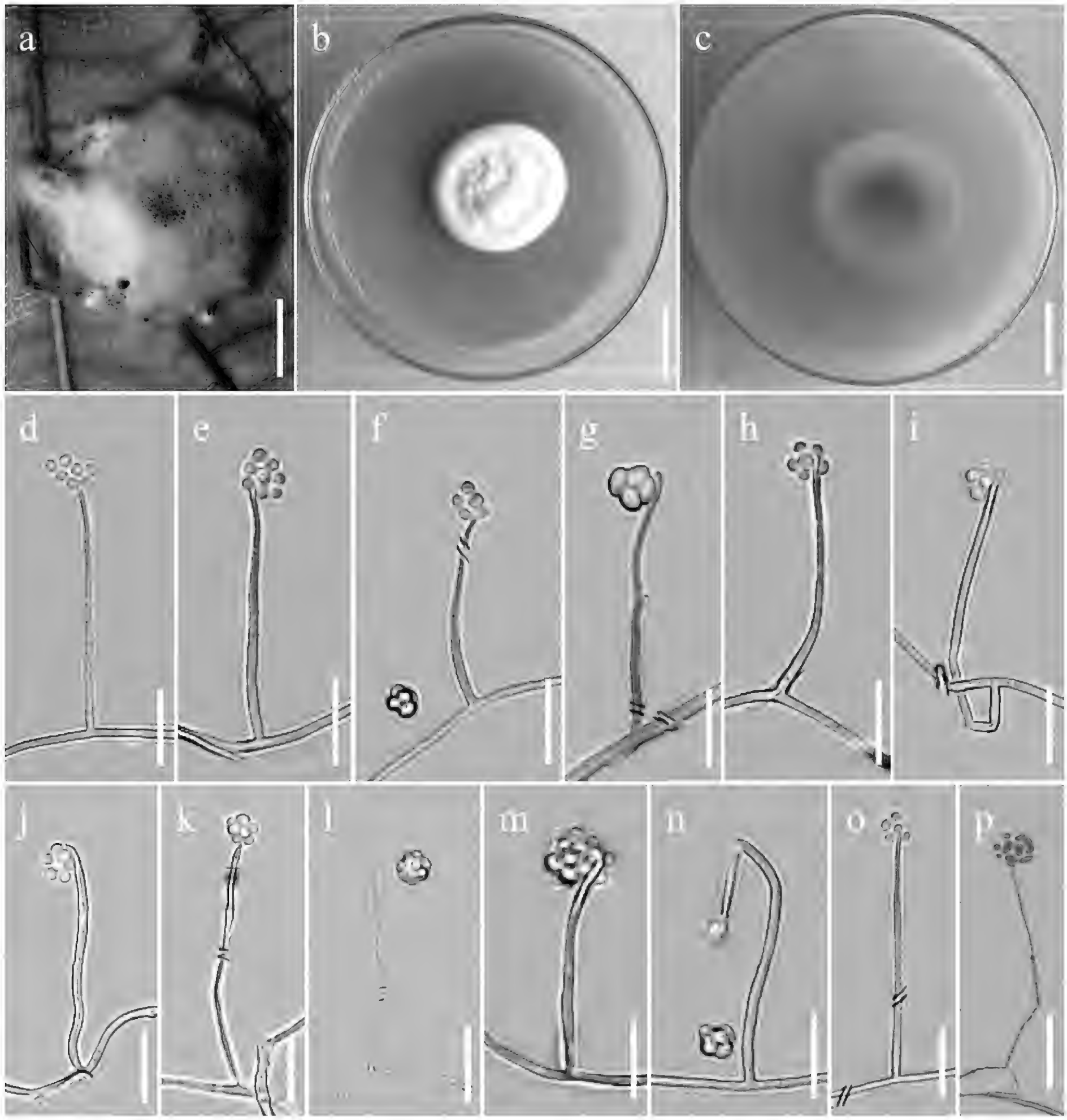

Figure 7. Morphology of *Simplicillium puwenense* **a** wild material **b** colonies obverse in PDA at 25 °C **c** colonies reverse on PDA at 25 °C **d–p** phialides bearing conidia. Scale bars: 3 mm (**a**); 3 cm (**b, c**); 10 μm (**d–f**); 8 μm (**g**); 10 μm (**h, i**); 12 μm (**j**); 10 μm (**k, l**); 8 μm (**m**); 10 μm (**n, o**); 15 μm (**p**).

***Asexual morph*.** Colonies on PDA medium moderate growth,diameter of 32–35 mm at 25 °C for 14 days, convex in middle surface, white fluffy to cotton like, dense, octahedral crystals absent, reverse brown to light brown with radial emission grooves. Hyphae septate, branched, transparent, with a diameter of 0.67–1.76 μm and smooth-walled. Cultures readily produced phialides and conidia after 14 days on PDA medium at room temperature. Phialides arising were slender, solitary, rod-shaped or columnar, measuring 3.37–52.57 μm in length and 0.5–1.6 μm in width. Conidia, transparent, single celled, smooth-walled, elliptical or oval or cylindrical, 1.19–2.41 × 0.88–1.6 μm. The conidia aggregated into a spherical shape at the top of the phialides, with a size of approximately 3.59–6.59 × 2.6–6.7 μm.

Host. Spider.

Distribution. China, Yunnan Province.

Additional material examined. CHINA • Yunnan Province, Honghe Hani and Yi autonomous prefecture, the Xilong Mountains. Specimens were collected from an evergreen broad-leaved forest, alt. 1,715 m, 102°32'48"E, 22°45'20"N, 1 June 2023, Jing Zhao (paratype: YHH SP2306001, ex-paratype living culture: YFCC 23069492); • Puwen Town,collected from an evergreen broad-leaved forest, alt. 1,019 m, 100°58'42"E, 22°31'10"N, 4 August 2023, Hong Yu (Specimen number: YHH SP2308001, Strain number: YFCC 23089322).

Remarks. Phylogenetically, three samples of *S. puwenense* were grouped together on a single branch, forming a monophyletic clade. It was identified as the sister species to *S. formicae*, supported by robust statistical evidence from both the Bayesian inference (BPP = 1) and the maximum likelihood analysis (BP = 100%). Both *S. puwenense* and *S. formicae* exhibited a stable topological structure with BP and BPP values of 100%. Morphologically, the surface of *S. puwenense* appeared centrally convex and exhibited a white, fluffy or cotton-like texture with densely arranged radial emission grooves ranging from reverse brown to light brown. Additionally, the conidia were observed to aggregate into spherical clusters at the apex of phialides (Table 2).

Table 2. Morphological comparisons of asexual morphs in the genus *Simplicillium*.

Species	Colony on PDA	Phialides (μm)	Conidia (μm)	Octahedral crystals	References
S. album	White, with a yellowish discharge, reverse beige to thick yellow, fluted	2–3 whorls or Solitary, 13.0–40.0 × 1.5–3.0 μm	Two conidia: macroconidia sickle-shaped or fusiform, 8.0–11.0 (–13.0) × 2.0–3.5 μm; Microconidia oval or oblong, 3.0–4.0 × 1.5–2.0 μm	Present	Zhang et al. (2021)
S. aogashimaense	White, reverse yellow white	Solitary, a few 2–3 whorls, slender and long (19–) 23–53 × 1.2–2.0 μm	Cylindrical, 4.2–6.5 × 1.2–2.0 (–2.3), conidia aggregate into spherical small heads at the top of bottle stem	Present	Nonaka et al. (2013)
S. araneae	White fluff, reverse yellow to brown	Solitary, slender, tapering from base to top, 32.9–47.1 × 1.2–2.4 μm	Subspherical, spherical, or elliptical, 1.8–2.9 × 1.2–1.8 μm	Absent	Chen et al. (2022)
S. calcicola	White or yellow, reverse light yellow to yellow	2–3 whorled or solitary, 14.0–38.0 × 1.0–2.0 μm	Two conidia: macroconidial fusiform, 4.5–8.0 × 1.0–2.0 μm; microconidia oval or globose or spherical, 2.0–3.5 × 1–1.5 μm	Absent	Zhang et al. (2017)
S. cicadellidae	White, reverse yellow	Solitary, 12.9–18.3 × 0.8–1.1 μm	Ellipsoid, 1.8–2.8 × 1.4–1.8 μm	Absent	Chen et al. (2019)
S. coccinellidae	White fluff, reverse yellow to light brown	Solitary, 4.9–62.1 × 1.0–1.5 μm	Subspherical or cylindrical or elliptical, 2.0–3.4 × 1.6–2.0 μm	Absent	Chen et al. (2021)
S. coleopterorum	White fluff, reverse light brown to brown	Solitary, 34.5–64.1 × 0.7–1.2 μm	Spherical or subspherical or elliptical, 2.1–3.3 × 1.5–1.9 μm	Absent	Chen et al. (2022)
S. cylindrosporum	White, reverse blond	2–3 whorled or solitary, 17–32 × 1.2–2.0 (–2.5) μm	Spherical or cylindrical, 3.0–4.5(–5.0) × 1.0–2.0 μm	Present	Nonaka et al. (2013)
S. formicidae	White, reverse light brown to brown, brown secretions	Solitary, 51–70.1 × 0.7–0.9 μm	Conidia aggregate into spherical slimy heads, mostly filamentous or fusiform, 3.9–7.9 × 0.8–1.3 μm	Absent	Chen et al. (2019)
S. guizhouense	White, reverse yellow to light yellow	Solitary, 1.1–52.2 × 1.0–1.8 μm	Oval or spherical, 2.4–2.9 × 1.6–1.8 μm	Absent	Chen et al. (2022)
S. humicola	White, light-yellow secretions, reverse light yellow to brown	2–3 whorled or solitary, 20.0–35.0 (–47.0) × 1.5–3.0 μm	Oblong or oval, 3.0–5.0 × 1.5–3.0 μm	Present	Zhang et al. (2021)
S. hymenopterorum	White, reserve light yellow	Mainly solitary, rarely whorls, 19.3–46.2 × 1.1–2.3 μm	Cylindrical to subellipsoidal, 2.1–2.8 × 1.3–1.9 μm, forming a subspherical small head at the top of the stem	Absent	Chen et al. (2021)
S. lamellicola	White, reserve light yellow	15–50 × 0.7–1.0 μm	Two conidia: macroconidia fusiform, 4.5–9.0 × 0.8–1.0 μm; microconidia ovoid to ellipsoid, 2.0–3.0 × 0.7–1.2 μm	Present	Zare and Gams (2001)

Species	Colony on PDA	Phialides (μm)	Conidia (μm)	Octahedral crystals	References
S. lanosoniveum	White or cream, reverse brownish cream to light yellow	Solitary, 20.0–40.0 × 1.1–2.0 μm	Spherical or ellipsoidal, 2.0–4.5 × 1.0–3.0 μm, forming a spherical or ellipsoidal tip at the top of the phialides,		Wei et al. (2019)
S. lepidopterorum	White, reserve light yellow	Solitary, 15.3–26.2 × 0.7–1.4 μm	Spindle-shaped or oval, 1.6– 2.4 × 1.4–1.7 μm, forming a slimy spherical head at the top of the phialides	Absent	Chen et al. (2019)
S. minatense	White, no secretion, reverse brown	Mainly solitary, rarely in whorls of 2–3, 11.0–31.0 (–47.0) × 1.0–1.7 μm	Spherical, 2.0–3.5 × 1.8–2.5 (–2.8) μm, forming a subglobose or ellipsoidal tip at the top of the phialides	Present	Nonaka et al. (2013)
S. neolepidopterorum	White, reverse yellow to light yellow	Solitary, 34.1–44.3 × 1.0–1.7 μm Solitary, 34.1–44.3 × 1.0–1.7 μm	Solitary, ellipsoidal to cylindrical, occasionally in short imbricate chains, 2.5–3.8 × 1.5–2.1 μm	Absent	Chen et al. (2021)
S. niveum	White	2–5 whorled, 10–20.5 (25.0) × 1–2 μm	Top growth, elongated or elliptical in shape, 3.0–4.5 (–6) × 1–2 μm		Crous et al. (2021)
S. pechmerlense	White, reverse light yellow to orange	Solitary, 16.0–31.0 × 0.9–1.2 μm	Two conidia: macroconidia fusiform, 5.0–8.0 × 1–1.6 μm; microconidia subglobular or elliptic, 1.8–3.0 × 0.9–1.5 μm, forming a slimy spherical head at the top of the phialides,	Absent	Leplat et al. (2021)
S. puwenense	**White fluffy to cotton like, convex in middle surface, reverse brown to light brown with radial emission grooves**	**Slender, solitary, rod-shaped or columnar, measuring 3.37–52.57 μm in length and 0.5–1.6 μm in width**	**Elliptical or oval or cylindrical, 1.19–2.41 × 0.88–1.6 μm. forming a spherical shape at the top of the phialides, 3.59–6.59 × 2.6–6.7 μm in size**	**Absent**	**This study**
S. scarabaeoidea	White, reverse light yellow	Solitary, 18.5–63.4 × 1.1–1.4 μm	Ellipsoidal, 1.9–2.9 × 1.4–2.0 μm	Absent	Chen et al. (2021)
S. subtropicum	White, reverse brownish orange to brown	(15.0–) 20–42 (–50.0) × 1.0–2.3 μm; Solitary, rarely in whorls of 2–3, (15.0–) 20.0–42.0 (–50.0) × 1.0–2.3 μm	Subglobose or ellipsoid, 2.3–4.0 (–4.5) × 1.5–3.3 μm, forming a spherical tip at the top of the phialides, 2.3–4.0 (–4.5) × 1.5–3.3 μm in size	Present	Nonaka et al. (2013)
S. sympodiophorum	White, reverse yellow white	2–4 whorled or solitary, 20.0–34 (–47.0) × 0.5–1.3 μm	Oval to ellipsoidal, 2.2–3.5 × 1.0–2.0 μm	Present	Nonaka et al. (2013)
S. yunnanense	White to light yellow, grayish orange to brown on back	Solitary, 5.8–16.9 × 1.1–1.5 μm	Cylindrical, 2.5–3.4 × 0.7–1.1 μm, conidia usually form chains at the top of the phialides	-	Wang et al. (2020)

Leptobacillium longiphialidum **Hong Yu bis, Y.L. Lu & Jing Zhao, sp. nov.**

MycoBank No: 856313

Fig. 8

Etymology. Referring to its longer phialides than those of the close relationship species in this genus.

Holotype. CHINA • Hainan Province, Qiongzhong City, Limushan Town, Limushan National Forest Park. Specimens were collected from an evergreen broad-leaved forest, alt. 589.9 m, 109°44'28"E, 19°10'41"N, 8 March 2023, Jing Zhao (***holotype*****:** YHH LL2303001, ***ex-type living culture*****:** YFCC 23039272).

Description. ***Sexual morph*****.** Not found.

Asexual morph**.** The colony was incubated at 25 °C on PDA medium for 14 days, the growth rate was slow, the diameter was 25–27 mm, the middle was fluffy to cotton, dense, convex and radial wrinkles, white and reverse brown to light yellow on the back. Mycelium branches, smooth walls, septate, transparent, with a diameter of approximately 0.97 × 1.72 μm. Cultures readily produced phialides and conidia after 10 days on PDA medium at room temperature. Phialides solitary, columnar, tapering from base to apex, 24.01–205.77 μm long, 1.00–2.24 μm wide. Conidia 2.88–4.54 × 1.18–1.95 μm, transparent, single celled in chains, smooth walls, narrow columnar or spindle-shaped, with apical conidia elliptical or nearly spherical in shape.

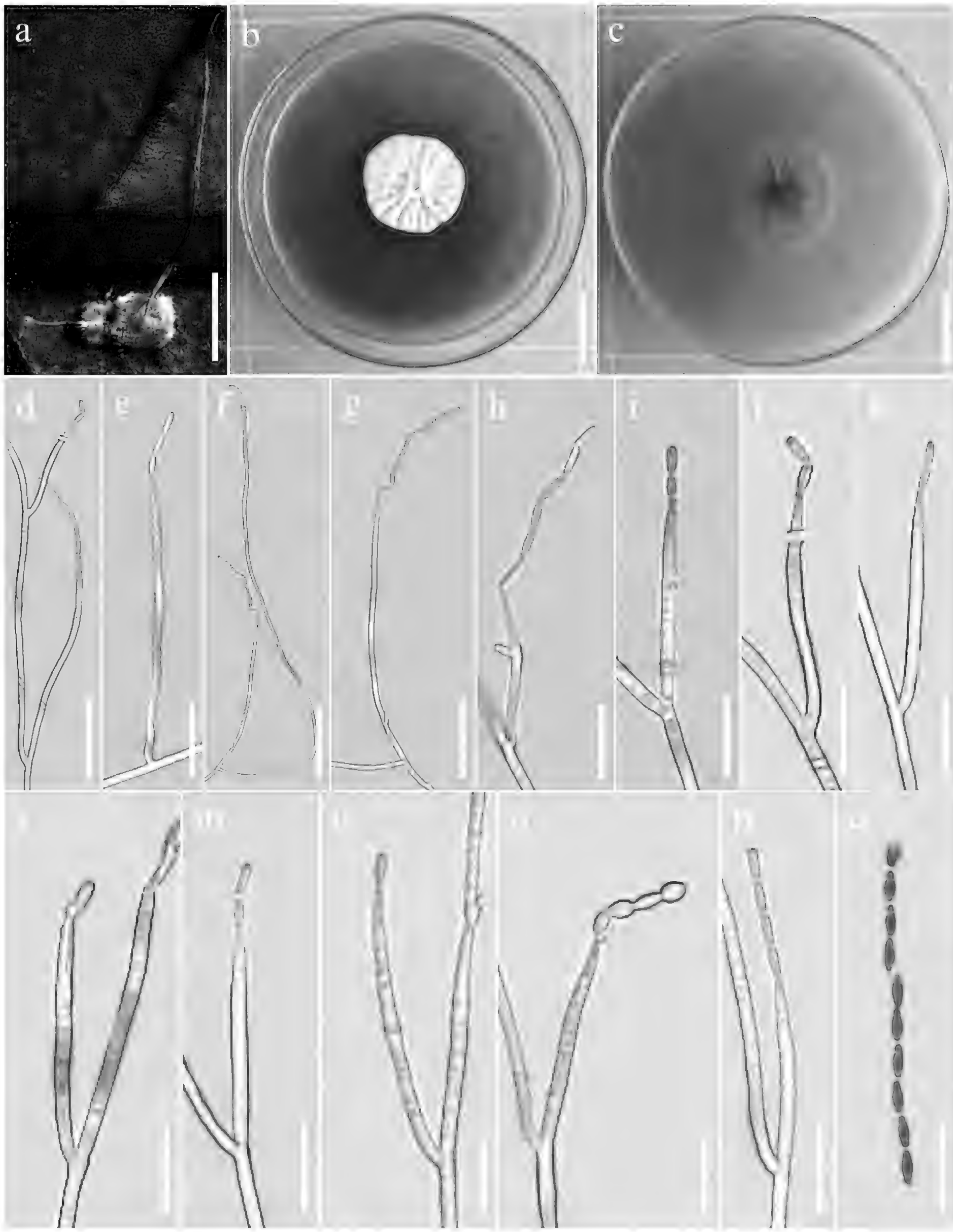

Figure 8. Morphology of *Leptobacillium longiphialidum* **a** wild material **b** colonies obverse in PDA at 25 °C **c** colonies reverse on PDA at 25 °C **d–p** phialides bearing conidia **q** conida. Scale bars: 2 mm (**a**); 2 cm (**b, c**); 20 μm (**d**); 12 μm (**e**); 30 μm (**f**); 20 μm (**g**); 10 μm (**h–k**); 9 μm (**l**); 10 μm (**m**); 7 μm (**n**); 8 μm (**o**); 10 μm (**p, q**).

Host. Spider.

Distribution. China, Hainan Province, Guangdong Province.

Additional material examined. CHINA • Guangdong Province, Huizhou City, Boluo County, 511 Township Road. Specimens were collected from an evergreen

Table 3. Morphological comparisons of asexual morphs in the genus *Leptobacillium*.

Species	Colony on PDA	Phialides (μm)	Conidia (μm)	References
L. cavernicola	White, reverse usually dark brown	Mainly solitary, slender, tapering toward tip, 5.1–27.2 × 1.2–1.7 μm	Forming long, slender chains, narrowly cylindrical to slightly fusiform, some were slightly lemon-shaped, first-formed conidium were usually shorter, obovoid to pyriform with a rounded distal end, 3.1–6.9 × 0.9–1.5 μm	Leplat et al. (2022)
L. chinense	White, reverse cream to light yellow	Solitary, (6.0–) 15–30 (–68.0) × 1.5 μm	Ellipsoidal or oval or cylindrical, 3.5–5.0 × 1.0–1.5 μm, the conidia aggregate into chains, with the apex conidia subspherical or obovoid, 1.5–2.5 × 1.5–2.0 μm	Liu and Cai (2012)
L. coffeanum	White, reverse cream	Solitary, few 2–3 whorls, 11.0–44.0 (–70.0) × 1.0–2.4 μm	Two conidia, macroconidia spindle-shaped, 5.3–8.8 × 1.0–1.6 μm; microconidia oval to fusiform, 2.2–3.8 × 0.8–1.5 μm	Gomes et al. (2018)
L. filiforme	White, reverse light yellow	Solitary, 9.0–18.0 × 1.0 μm	Fusiform to filamentous, chained, sometimes forming zigzag chains, 7.2–12.5 × 1.0 μm	Crous et al. (2018)
L. latisporum	White, reverse greyish orange to orange white	13.2–40.8 × 2.9–4.8 μm	Shuttle shaped to narrow cylindrical, with single cells forming long chains, 3.9–6.3 × 1.9–3.9 μm	Preedanon et al. (2023)
L. longiphialidum	**White, reverse brown to light yellow**	**Solitary, 24.01–205.77 × 1.00–2.24 μm**	**Narrow columnar or spindle shaped, 2.88–4.54 × 1.18–1.95 μm, single celled in chains, with apical conidia elliptical or nearly spherical in shape**	**This study**
L. leptobactrum var. *calidius*	White to cream, reverse Light yellow to brown	Solitary, few 1–2 whorls, 18.4–60.0 × 0.7–2.0 μm	Narrow cylindrical (rod-shaped) to slightly fusiform, 3.0–5.7 × 0.7–1.7 μm	Zare and Gams (2016)
L. leptobactrum var. *leptobactrum*	White to cream, reverse Light yellow to yellowish brown	15.8–31.7 × 0.7–1.5 μm Solitary, few 2–3 whorls, 15.8–31.7 × 0.7–1.5 μm	Narrow rod-shaped or narrow cylindrical (rod-shaped), 3.0–6.1 × 0.8–2.1 μm	Zare and Gams (2016)
L. leptobactrum	White, gray white to pinkish white, reverse orange to orange brown, gray white, light yellow, milky white to dark yellow	Solitary, few 1–2 branches, 20.0–45.0 μm long, Base width 1–2 μm, top width 0.5–0.7 μm	Narrow cylindrical (rod-shaped) to slightly fusiform, 4.5–8.0 × 0.8–1.5 (–2.0) μm	Zare and Gams (2016)
L. muralicola	White, gray white to green white, reverse light yellow, milky white to dark yellow, orange to orange brown, ochraceous	Solitary, few 1–2 branches, 20.0–45.0 μm long, Base width 1.0–2.0 μm, top width 0.5–0.7 μm	Narrow cylindrical (rod-shaped) to slightly fusiform, 4.5–6.0 × 1.0–2.0 μm	Sun et al. (2019)
L. symbioticum	White, reverse orange yellow to orange-brown	Solitary, few 2–3 whorls, 7.1–30.6 × 1.6–3.5 μm	Slightly fusiform to narrowly cylindrical, 4.0–6.9 × 0.7–1.6 μm	Okane et al. (2020)

broad-leaved forest, alt. 29.4 m, 114°24'5"E, 23°14'32"N, 23 July 2024, Hong Yu and Y.L. Lu (paratype: YHH LL2407001, ex-paratype living culture: YFCC 24079491.

Remarks. The key characteristic of *L. longiphialidum* was its independent, columnar shape and the presence of narrow or fusiform spores. Phylogenetic analyses showed that *L. longiphialidum* belonged to the *Leptobacillium* clade and was closest to *L. marksiae*. However, the host and collection sites of *L. longiphialidum* were spiders and China, respectively and the host and collection sites of *L. marksiae* were an unidentified dead insect and Queensland, Australia, respectively. *L. longiphialidum* and *L. marksiae* were distinguished by genetic distance. (Table 3).

Discussion

The genera of *Simplicillium* and *Leptobacillium* were found to be the most closely related within the family of Cordycipitaceae. They exhibited a wide distribution and were commonly observed on various substrates or hosts, including air, seawater, rocks, leaves, soil, insects, fungi, freshwater environments, murals, rocks and caves (Liu and Cai 2012; Zare and Gams 2016; Crous et al. 2018; Gomes et al. 2018; Sun et al. 2019; Wei et al. 2019; Kondo et al. 2020; Okane et al. 2020; Wang et al. 2020;

Leplat et al. 2021). Chen et al. (2019) first reported insect-associated species of *Simplicillium* while later reporting an additional eight arthropod-related species of the genus *Simplicillium* (Chen et al. 2021, 2022). Furthermore, Leplat et. al (2022) isolated *L. cavernicola* Leplat from caves as a representative species of the genus *Leptobacillium* whereas *L. muralicola* Z. Sun, Qin Y. Ge, Zhi B. Zhu & Xing Z. Liu was isolated from mural paintings in a Koguryo tomb in China (Sun et al. 2019).

The macroscopic and microscopic morphology of most species in the genera of *Simplicillium* and *Leptobacillium* are quite similar and it is difficult to distinguish specific species, based on only morphological features. Thus, it is often necessary to combine morphological and molecular data for species identification. The utilisation of ITS and nrLSU by Liu and Cai (2012) yielded more accurate outcomes in the identification of *Simplicillium* species. To date, multi-site phylogenies incorporating the combined analysis of ribosomal DNA and functional protein-coding genes have been extensively employed in fungal phylogeny research, yielding numerous significant findings (Sung et al. 2007; Luangsa-ard et al. 2017; Mongkolsamrit et al. 2020; Wang et al. 2020). The results showed that the molecular phylogenies of *Simplicillium* and *Lecanicillium*, based on ITS fragment, nrLSU fragment and six-gene combined dataset, were more stable in topology. This was consistent with the results of previous studies. In this study, two novel species, *S. puwenense* and *L. longiphialidum*, were identified and characterised through meticulous morphological examination and rigorous phylogenetic analysis.

Through morphological observation, it was found that phialides of species in the genus of *Simplicillium* were solitary and could be distinguished from those of the genus of *Lecanicillium* (Chen et al. 2021). It was observed that a prominent characteristic of species within the *Simplicillium* genus was the solitary nature of phialides, wherein conidia typically adhered to the apex of phialides in chains exhibiting spherical, sticky, or tile-like properties, ultimately resulting in the formation of octahedral crystals (Zare and Gams 2001). The primary distinguishing feature of *Leptobacillium* species lay in the presence of two conidia; single cells arranged in clusters with near-spherical or elliptical conidia at the apex and other narrow columnar (rod) to fusiform-shaped conidia (Zare and Gams 2016; Leplat et al. 2022). The phialides of *S. puwenense* collected in this study were slender, solitary, rod-shaped or columnar; the conidia were transparent, single-celled with smooth walls and had an oval or cylindrical shape. They formed aggregates into a spherical structure at the apex of the phialides. These characteristics aligned closely with the primary identification features described for *Simplicillium* species by Zare and Gams (2001). The phialides of *L. longiphialidum* appeared as solitary and columnar structures. Two types of conidia were observed, i.e. one type consisted of single cells clustered together in chains, while the other type was oval or nearly spherical and located at the apex. Additionally, there was another type of narrow columnar or spindle-shaped conidium present, which was consistent with previous studies on *Leptobacillium* species (Zare and Gams 2016; Leplat et al. 2022).

In phylogenetic trees, most species of the genera *Simplicillium* and *Leptobacillium* were clustered in their separate clades and were well supported and topologically stable. However, the phylogenetic framework showed that two samples of *L. leptobactrum*, ZJ14B02 and AH17C05, did not form a monophyletic clade. The ITS sequence and nrLSU sequence of strain ZJ14B02 contained 547 bp and 909 bp, respectively. The ITS and nrLSU sequences of

strain AH17C05 contained 557 bp and 929 bp, respectively. It was found that the head and tail bases of ITS sequence of samples ZJ14B02 and AH17C05 were different from those of nrLSU sequences. It was speculated that the two samples of *L. leptobactrum* did not form a monophyletic clade, which might be caused by the poor processing of the fore-tail primer sequence. Zare and Gams (2016) initially described *L. leptobactrum*, composed of *L. leptobactrum* var. *leptobactrum* and *L. leptobactrum* var. *calidius*, which were distinguished by their optimal growth temperature. The optimum temperature for growth of *L. leptobactrum* var. *leptobactrum* was 18–21 °C, no growth at 30 °C (Zare and Gams 2016). The optimum temperature for growth of *L. leptobactrum* var. *calidius* was 24–27 °C, reduced growth at 30 °C, no growth at 33 °C (Zare and Gams 2016). Phylogenetic studies had placed two strains in unexpected clades, namely *L. leptobactrum* var. *leptobactrum* and *L. leptobactrum* var. *calidius*. In the phylogenetic framework constructed by nrSSU, *L. leptobactrum* var. *leptobactrum* and *L. leptobactrum* var. *calidius* clustered into a clade. The findings of phylogenetic frameworks, based on ITS, nrLSU and six-gene datasets, revealed that *L. leptobactrum* var. *calidius* and *L. chinense* formed a cluster, while *L. leptobactrum* var. *leptobactrum* and *L. cavernicola* also clustered together. This was consistent with the findings of Leplat et al. (2022).

S. pechmerlense J. Leplat constituted an independent clade that exhibited slight differences compared to the previously studied phylogenetic framework (Leplat et al. 2021). However, it was the same as the phylogenetic framework reconstructed by Chen et al. (2022). Additionally, Leplat et al. (2021) found that the underside of the colony of *S. pechmerlense* was light yellow to orange, the phialides was solitary and there were two kinds of conidium, the macroconidia was spindle, 5.0–8.0 × 1.0–1.6 µm. The microconidia were subspherical or elliptic, 1.8–3.0 × 0.9–1.5 µm, forming slimy globular heads at the top of the phialides. *S. pechmerlense* phialides solitary and conidia attached to the top of the phialides with slimy heads fit the main identification characteristics of *Simplicillium* (Zare and Gams 2001). *S. pechmerlense* was morphologically similar to *S. calcicola* Z.F. Zhang, F. Liu & L. Cai and *S. album* Z.F. Zhang & L. Cai (Leplat et al. 2021). The phialides of *S. calcicola* and *S. album* were 2–3-whorled or solitary (Zhang et al. 2017, 2021), while *S. pechmerlense* were solitary. The solitary phialides could distinguish *S. pechmerlense* from *S. calcicola* and *S. album*. Species of *Simplicillium* have frequently been identified using ITS and nrLSU sequences (Liu and Cai 2012). Phylogenetic analyses, based on single gene fragments revealed an unstable systematic position for *S. pechmerlense*. However, the morphological characteristics of *S. pechmerlense* align with the primary identification features of *Simplicillium*. Consequently, it was determined that *S. pechmerlense* should be retained within the genus *Simplicillium*. The inclusion of supplementary materials, such as morphological data, would be essential for further verification since only one strain of polygenic sequence data was available for *L. leptobactrum* var. *leptobactrum* and *L. leptobactrum* var. *calidius*.

Acknowledgements

Many thanks to Peng Ronghua of Guangdong Small Worm Biotechnology Co., Ltd. for his help in this study. At the same time, we also thank the two reviewers and editors for their critiques and suggestions which greatly improved our manuscript.

Additional information

Conflict of interest

The authors have declared that no competing interests exist.

Ethical statement

No ethical statement was reported.

Funding

This work was supported by the National Natural Science Foundation of China (32200013) and supported by the Research and Innovation Fund for Graduate Students of Yunnan University (KC-23235594).

Author contributions

Yingling Lu: Responsible for investigation, article conception, writing and editing, and species identification; Songyu Li: Responsible for investigation, article conception, writing and editing, morphological analysis and phylogenetic analysis; Zuoheng Liu: Collecting the information of specimens and GenBank entry number required for research; Jing Zhao: Responsible for picture editing and processing; Zhiyong Yu, Zongli Liang, Hailong He, Jianhong Li, Yun Huang, Xinming Li: Responsible for investigation; Hong Yu: Responsible for investigation, conceptualisation, writing – review and editing and supervision.

Author ORCIDs

Yingling Lu https://orcid.org/0009-0008-8119-1975
Songyu Li https://orcid.org/0009-0007-9589-0892
Zuoheng Liu https://orcid.org/0000-0003-4118-3694
Jing Zhao https://orcid.org/0000-0001-7871-2209
Zhiyong Yu https://orcid.org/0000-0001-8276-5901
Zongli Liang https://orcid.org/0009-0006-5553-8811
Hailong He https://orcid.org/0009-0000-7862-0865
Jianhong Li https://orcid.org/0009-0001-1234-7816
Yun Huang https://orcid.org/0009-0007-3429-1490
Xinming Li https://orcid.org/0009-0001-7198-281X
Hong Yu https://orcid.org/0000-0002-2149-5714

Data availability

All of the data that support the findings of this study are available in the main text.

References

Bischoff JF, Rehner SA, Humber RA (2006) *Metarhizium frigidum* sp. nov.: A cryptic species of *M. anisopliae* and a member of the *M. flavoviride* Complex. Mycologia 98(5): 737–745. https://doi.org/10.1080/15572536.2006.11832645

Chen WH, Liu C, Han YF, Liang JD, Tian WY, Liang ZQ (2019) Three novel insect-associated species of *Simplicillium* (Cordycipitaceae, Hypocreales) from Southwest China. MycoKeys 58: 83–102. https://doi.org/10.3897/mycokeys.58.37176

Chen WH, Han YF, Liang JD, Liang ZQ (2021) Taxonomic and phylogenetic characterizations reveal four new species of *Simplicillium* (Cordycipitaceae, Hypocreales) from Guizhou, China. Scientific Reports 11(1): 15300. https://doi.org/10.1038/s41598-021-94893-z

Chen W, Liang J, Ren X, Zhao J, Han Y, Liang Z (2022) Multigene phylogeny, phylogenetic network, and morphological characterizations reveal four new arthropod-associated *Simplicillium* species and their evolutional relationship. Frontiers in Microbiology 13: 950773. https://doi.org/10.3389/fmicb.2022.950773

Crous P, Luangsa-Ard J, Wingfield M, Carnegie A, Hernández-Restrepo M, Lombard L, Roux J, Barreto R, Baseia I, Cano Lira J, Martín MP, Morozova OV, Stchigel AM, Summerell BA, Brandrud TE, Dima B, García D, Giraldo A, Guarro J, Gusmão LFP, Khamsuntorn P, Noordeloos ME, Nuankaew S, Pinruan U, Rodríguez-Andrade E, Souza-Motta CM, Thangavel R, van Iperen AL, Abreu VP, Accioly T, Alves JL, Andrade JP, Bahram M, Baral H-O, Barbier E, Barnes CW, Bendiksen E, Bernard E, Bezerra JDP, Bezerra JL, Bizio E, Blair JE, Bulyonkova TM, Cabral TS, Caiafa MV, Cantillo T, Colmán AA, Conceição LB, Cruz S, Cunha AOB, Darveaux BA, da Silva AL, da Silva GA, da Silva GM, da Silva RMF, de Oliveira RJV, Oliveira RL, De Souza JT, Dueñas M, Evans HC, Epifani F, Felipe MTC, Fernández-López J, Ferreira BW, Figueiredo CN, Filippova NV, Flores JA, Gené J, Ghorbani G, Gibertoni TB, Glushakova AM, Healy R, Huhndorf SM, Iturrieta-González I, Javan-Nikkhah M, Juciano RF, Jurjević Ž, Kachalkin AV, Keochanpheng K, Krisai-Greilhuber I, Li Y-C, Lima AA, Machado AR, Madrid H, Magalhães OMC, Marbach PAS, Melanda GCS, Miller AN, Mongkolsamrit S, Nascimento RP, Oliveira TGL, Ordoñez ME, Orzes R, Palma MA, Pearce CJ, Pereira OL, Perrone G, Peterson SW, Pham THG, Piontelli E, Pordel A, Quijada L, Raja HA, Rosas de Paz E, Ryvarden L, Saitta A, Salcedo SS, Sandoval-Denis M, Santos TAB, Seifert KA, Silva BDB, Smith ME, Soares AM, Sommai S, Sousa JO, Suetrong S, Susca A, Tedersoo L, Telleria MT, Thanakitpipattana D, Valenzuela-Lopez N, Visagie CM, Zapata M, Groenewald JZ (2018) Fungal Planet description sheets: 785–867. Persoonia 41(1): 238–417. https://doi.org/10.3767/persoonia.2018.41.12

Crous PW, Cowan DA, Maggs-Kölling G, Yilmaz N, Thangavel R, Wingfield MJ, Noordeloos ME, Dima B, Brandrud TE, Jansen GM, Morozova OV, Vila J, Shivas RG, Tan YP, Bishop-Hurley S, Lacey E, Marney TS, Larsson E, Le Floch G, Lombard L, Nodet P, Hubka V, Alvarado P, Berraf-Tebbal A, Reyes JD, Delgado G, Eichmeier A, Jordal JB, Kachalkin AV, Kubátová A, Maciá-Vicente JG, Malysheva EF, Papp V, Rajeshkumar KC, Sharma A, Spetik M, Szabóová D, Tomashevskaya MA, Abad JA, Abad ZG, Alexandrova AV, Anand G, Arenas F, Ashtekar N, Balashov S, Bañares Á, Baroncelli R, Bera I, Biketova AY, Blomquist CL, Boekhout T, Boertmann D, Bulyonkova TM, Burgess TI, Carnegie AJ, Cobo-Diaz JF, Corriol G, Cunnington JH, da Cruz MO, Damm U, Davoodian N, de A Santiago ALCM, Dearnaley J, de Freitas LWS, Dhileepan K, Dimitrov R, Di Piazza S, Fatima S, Fuljer F, Galera H, Ghosh A, Giraldo A, Glushakova AM, Gorczak M, Gouliamova DE, Gramaje D, Groenewald M, Gunsch CK, Gutiérrez A, Holdom D, Houbraken J, Ismailov AB, Istel Ł, Iturriaga T, Jeppson M, Jurjević Ž, Kalinina LB, Kapitonov VI, Kautmanová I, Khalid AN, Kiran M, Kiss L, Kovács Á, Kurose D, Kušan I, Lad S, Læssøe T, Lee HB, Luangsa-Ard JJ, Lynch M, Mahamedi AE, Malysheva VF, Mateos A, Matočec N, Mešić A, Miller AN, Mongkolsamrit S, Moreno G, Morte A, Mostowfizadeh-Ghalamfarsa R, Naseer A, Navarro-Ródenas A, Nguyen TTT, Noisripoom W, Ntandu JE, Nuytinck J, Ostrý V, Pankratov TA, Pawłowska J, Pecenka J, Pham THG, Polhorský A, Pošta A, Raudabaugh DB, Reschke K, Rodríguez A, Romero M, Rooney-Latham S, Roux J, Sandoval-Denis M, Smith MT, Steinrucken TV, Svetasheva TY, Tkalčec Z, van der Linde EJ, V D Vegte M, Vauras J, Verbeken A, Visagie CM, Vitelli JS, Volobuev SV, Weill A, Wrzosek M, Zmitrovich IV, Zvyagina EA, Groenewald JZ (2021) Fungal Planet description sheets: 1182–1283. Persoonia 46: 313–528. https://doi.org/10.3767/persoonia.2021.46.11

Gomes AA, Pinho DB, Cardeal Z, Menezes HC, De Queiroz MV, Pereira OL (2018) *Simplicillium coffeanum*, a new endophytic species from Brazilian coffee plants, emitting

antimicrobial volatiles. Phytotaxa 333(2): 188–198. https://doi.org/10.11646/phytotaxa.333.2.2

Kepler RM, Luangsa-Ard JJ, Hywel-Jones NL, Quandt CA, Sung GH, Rehner SA, Aime MC, Henkel TW, Sanjuan T, Zare R, Chen M, Li Z, Rossman AY, Spatafora JW, Shrestha B (2017) A phylogenetically-based nomenclature for Cordycipitaceae (Hypocreales). IMA Fungus 8(2): 335–353. https://doi.org/10.5598/imafungus.2017.08.02.08

Kondo N, Iwasaki H, Tokiwa T, Mura S, Nonaka K (2020) *Simplicillium spumae* (Cordycipitaceae, Hypocreales), a new hyphomycetes from aquarium foam in japan. Mycoscience 61(3): 116–121. https://doi.org/10.1016/j.myc.2020.02.002

Leplat J, Francois A, Bousta F (2021) *Simplicillium pechmerlensis*, a new fungal species isolated from the air of the Pech-Merle show cave. Phytotaxa 521(2): 80–94. https://doi.org/10.11646/phytotaxa.521.2.2

Leplat J, Francois A, Bousta F (2022) *Leptobacillium cavernicola*, a newly discovered fungal species isolated from several Paleolithic-decorated caves in France. Phytotaxa 571(2): 186–196. https://doi.org/10.11646/phytotaxa.571.2.5

Liu F, Cai L (2012) Morphological and molecular characterization of a novel species of *Simplicillium* from China. Cryptogamie Mycologie 33(2): 137–144. https://doi.org/10.7872/crym.v33.iss2.2012.137

Liu ZY, Liang ZQ, Whalley AJS, Yao YJ, Liu AY (2001) *Cordyceps brittlebankisoides*, a new pathogen of grubs and its anamorph, *Metarhizium anisopliae* var. *majus*. Journal of Invertebrate Pathology 78(3): 178–182. https://doi.org/10.1006/jipa.2001.5039

Luangsa-ard JJ, Mongkolsamrit S, Thanakitpipattana D, Khonsanit A, Tasanathai K, Noisripoom W, Humber RA (2017) Clavicipitaceous entomopathogens: new species in *Metarhizium* and a new genus *Nigelia*. Mycological Progress 16(4): 369–391. https://doi.org/10.1007/s11557-017-1277-1

Mongkolsamrit S, Noisripoom W, Thanakitpipattana D, Wutikhun T, Spatafora JW, Luangsa-Ard J (2018) Disentangling cryptic species with *Isaria*-like morphs in Cordycipitaceae. Mycologia 110(1): 230–257. https://doi.org/10.1080/00275514.2018.1446651

Mongkolsamrit S, Khonsanit A, Thanakitpipattana D, Tasanathai K, Noisripoom W, Lamlertthon S, Himaman W, Houbraken J, Samson RA, Luangsa-ard J (2020) Revisiting *Metarhizium* and the description of new species from Thailand. Studies in Mycology 95(1): 171–251. https://doi.org/10.1016/j.simyco.2020.04.001

Nonaka K, Kaifuchi S, Ōmura S, Masuma R (2013) Five new *Simplicillium* species (Cordycipitaceae) from soils in Tokyo, Japan. Mycoscience 54(1): 42–53. https://doi.org/10.1016/j.myc.2012.07.002

Okane I, Nonaka K, Kurihara Y, Abe JP, Yamaoka Y (2020) A new species of *Leptobacillium*, *L. symbioticum*, isolated from mites and sori of soybean rust. Mycoscience 61(4): 165–171. https://doi.org/10.1016/j.myc.2020.04.006

Preedanon S, Suetrong S, Srihom C, Somrithipol S, Kobmoo N, Saengkaewsuk S, Srikitikulchai P, Klaysuban A, Nuankaew S, Chuaseeharonnachai C, Chainuwong B, Muangsong C, Zhang ZF, Cai L, Boonyuen N (2023) Eight novel cave fungi in Thailand's Satun Geopark. Fungal Systematics and Evolution 12(1): 1–30. https://doi.org/10.3114/fuse.2023.12.01

Regaieg H, Ciancio A, Raouani NH, Rosso L (2011) Detection and biocontrol potential of *Verticillium leptobactrum* parasitizing *Meloidogyne* spp. World Journal of Microbiology and Biotechnology 27(7): 1615–1623. https://doi.org/10.1007/s11274-010-0615-0

Rehner SA, Samuels GJ (1994) Taxonomy and phylogeny of Glio cladium analysed from nuclear large subunit ribosomal DNA sequences. Mycological Research 98(6): 625–634. https://doi.org/10.1016/S0953-7562(09)80409-7

Rehner SA, Minnis AM, Sung GH, Luangsa-ard JJ, Devotto L, Humber RA (2011) Phylogeny and systematics of the anamorphic, entomopathogenic genus *Beauveria*. Mycologia 103(5): 1055–1073. https://doi.org/10.3852/10-302

Sun JZ, Ge QY, Zhu ZB, Zhang XL, Liu XZ (2019) Three dominating hypocrealean fungi of the 'white mold spots' on acrylic varnish coatings of the murals in a Koguryo tomb in China. Phytotaxa 397(3): 225–236. https://doi.org/10.11646/phytotaxa.397.3.2

Sung GH, Hywel-Jones NL, Sung JM (2007) Phylogenetic classification of Cordyceps and the clavicipitaceous fungi. Studies in Mycology 57: 5–59. https://doi.org/10.3114/sim.2007.57.01

Vilgalys R, Hester M (1990) Rapid genetic identification and mapping of enzymatically amplified ribosomal DNA from several *Cryptococcus* species. Journal of Bacteriology 172(8): 4238–4246. https://doi.org/10.1128/jb.172.8.4238-4246.1990

Wang YB, Yu H, Dai YD, Chen ZH, Zeng WB, Yuan F, Liang ZQ (2015a) *Polycephalomyces yunnanensis* (Hypocreales), a new species of *Polycephalomyces* parasitizing *Ophiocordyceps* nutans and stink bugs (hemipteran adults). Phytotaxa 208: 034–044.

Wang YB, Yu H, Dai YD, Wu CK, Zeng WB, Yuan F, Liang ZQ (2015b) Polycephalomyces agaricus, a new hyperparasite of *Ophiocordyceps* sp. infecting melolonthid larvae in southwestern China. Mycological Progress 14(9): 70. https://doi.org/10.1007/s11557-015-1090-7

Wang YB, Wang Y, Fan Q, Duan DE, Zhang GD, Dai RQ, Dai YD, Zeng WB, Chen ZH, Li DD, Tang DX, Xu ZH, Sun T, Nguyen T, Tran N, Dao V, Zhang CM, Huang LD, Liu YJ, Zhang XM, Yang DR, Sanjuan T, Liu XZ, Yang ZL, Yu H (2020) Multigene phylogeny of the family Cordycipitaceae (Hypocreales): New taxa and the new systematic position of the Chinese cordycipitoid fungus *Paecilomyces hepiali*. Fungal Diversity 103: 1–46. https://doi.org/10.1007/s13225-020-00457-3

Wei DP, Wanasinghe DN, Hyde KD, Mortimer PE, Xu J, Xiao YP, Bhunjun CS, To-Anun C (2019) The genus *Simplicillium*. MycoKeys 60: 69–92. https://doi.org/10.3897/mycokeys.60.38040

White TJ, Bruns TD, Lee SB, Taylor JW (1990) Amplification and direct sequencing of fungal ribosomal RNA genes for phylogenet ics. In: Innis MA, Gelfand DH, Sninsky JJ, White TJ (Eds) PCR protocols: a guide to methods and applications. Academic, New York, 315–322. https://doi.org/10.0000/PMID1793

Yan QH, Ni QR, Gu WJ, Liu HW, Yuan XY, Sun JZ (2023) *Simplicillium sinense* sp. nov., a novel potential pathogen of tinea faciei. Frontiers in Microbiology 14: 1156027. https://doi.org/10.3389/fmicb.2023.1156027

Zare R, Gams W (2001) A revision of *Verticillium* section *Prostrata*. IV. The genera *Lecanicillium* and *Simplicillium* gen. nov. Nova Hedwigia 73(1–2): 1–50. https://doi.org/10.1127/nova.hedwigia/73/2001/1

Zare R, Gams W (2008) A revision of the *Verticillium fungicola* species complex and its affinity with the genus *Lecanicillium*. Mycological Research 112(7): 811–824. https://doi.org/10.1016/j.mycres.2008.01.019

Zare R, Gams W (2016) More white verticillium-like anamorphs with erect conidiophores. Mycological Progress 15(10–11): 993–1030. https://doi.org/10.1007/s11557-016-1214-8

Zhang ZF, Liu F, Zhou X, Liu XZ, Liu SJ, Cai L (2017) Culturable mycobiota from Karst caves in China, with descriptions of 20 new species. Persoonia 39(1): 1–31. https://doi.org/10.3767/persoonia.2017.39.01

Zhang ZF, Zhou SY, Eurwilaichitr L, Ingsriswang S, Raza M, Chen Q, Zhao P, Liu F, Cai L (2021) Culturable mycobiota from Karst caves in China II, with descriptions of 33 new species. Fungal Diversity 106(1): 29–136. https://doi.org/10.1007/s13225-020-00453-7